Band structure renormalization and weak pseudogap behavior in $Na_{0.33}CoO_2$: Fluctuation exchange study based on a single-band model

Zi-Jian Yao,[1,2] Jian-Xin Li,[1] and Z. D. Wang[2,1]
[1]*National Laboratory of Solid State Microstructures and Department of Physics, Nanjing University, Nanjing 210093, China*
[2]*Department of Physics and Center of Theoretical and Computational Physics, The University of Hong Kong, Pokfulam Road, Hong Kong, China*

(Received 27 August 2007; revised manuscript received 5 November 2007; published 19 December 2007)

Based on a single-band Hubbard model and the fluctuation exchange approximation, the effective mass and the energy band renormalization in $Na_{0.33}CoO_2$ is elaborated. The renormalization is observed to exhibit certain kind of anisotropy, which agrees qualitatively with the angle-resolved photoemission spectroscopy measurements. Moreover, the spectral function and density of states in the normal state are calculated, with a weak pseudogap behavior being seen, which is explained as a result of the strong Coulomb correlations. Our results suggest that the large Fermi surface associated with the a_{1g} band plays likely a central role in the charge dynamics.

DOI: 10.1103/PhysRevB.76.212506 PACS number(s): 74.70.−b, 71.18.+y, 71.27.+a, 74.25.Jb

The layered oxide Na_xCoO_2 has attracted much attention due to its possible connection to the high-T_c superconductivity since the discovery of superconductivity in it.[1,2] This material consists of two-dimensional CoO_2 layers, where Co form a triangular lattice, making the Na_xCoO_2 a possible realization of Anderson's resonating valence bond state.[3] By hydration, it becomes a superconductor with $T_c \approx 5$ K in $Na_{0.35}CoO_2 \cdot 1.3H_2O$.[1] The unhydrated compound Na_xCoO_2 exhibits a rich phase diagram: a paramagnetic metal ($x < 0.5$), a charge-ordered insulator ($x=0.5$), a "Curie-Weiss metal" ($x \sim 0.7$), and a magnetic order state ($x \geqq 0.75$).[4]

Experimentally, it is indicated that Na_xCoO_2 seems to be strongly electronic correlated.[2,5,6] Angle-resolved photoemission spectroscopy (ARPES) measurements show a strong mass renormalization (the effective mass is about five to ten times larger than the bare mass) for $x=0.6$.[7] Decreasing the Na concentration to $x=0.3$, the cobaltates appear to be less electron correlated with a weaker but still apparent energy band renormalization factor (~ 2).[8] For the hydrated compounds, the effective mass is estimated to be $\sim 2-3$.[9] In addition, recent experiments report that $Na_{0.33}CoO_2 \cdot 1.3H_2O$ display certain pseudogap behaviors such as the decreasing of the Knight shift[10] and the density of states (DOS) at the Fermi level below 300 K.[11] Optical spectroscopy measurements for $Na_{0.2}CoO_2$ and $Na_{0.5}CoO_2$ also suggest the incipient formation of pseudogap.[12] However, unlike the pseudogap effect observed in the high-T_c cuprates, the pseudogap behavior here is rather weak. The renormalization of the energy band and the pseudogap formation are directly related to the electronic structure, such as the quasiparticle spectral function, the quasiparticle dispersion, and the Fermi surface (FS) topology. Therefore, it is of importance and significance to study the normal state quasiparticle dynamics.

It is believed that the topology of the FS plays an important role in the unconventional superconductivity. The local density approximation (LDA) calculations[13,14] predict a large FS associated with the a_{1g} band and six pockets associated with the e_g' band. However, intriguingly, the small pockets have not been observed in the ARPES measurements.[8,9,15] The unexpected inconsistency of the topology of the FS between the LDA results and the ARPES measurements has aroused much controversy. One possibility might be due to the surface effect in the ARPES measurements. From another viewpoint, Zhou *et al.* suggested that the strong Coulomb interactions may induce significant renormalization of the band structure which pulls the e_g' band down from the Fermi energy.[16] Furthermore, the e_g' band is suggested to be relevant to the spin-triplet superconductivity in some theoretical and numerical studies.[17,18] On the other hand, the possibility of the spin-singlet superconductivity is also suggested according to recent Knight-shift measurements.[19,20] Taking the above considerations into account, a single-band model focusing on the a_{1g} band may be a starting point as a minimal model of Na_xCoO_2.

In this Brief Report, we study the normal state electronic structure in $Na_{0.33}CoO_2$ on the basis of the single-band Hubbard model and the fluctuation exchange (FLEX) approximation. Several experimental features, such as the band renormalization and the weak pseudogap behavior, are well reproduced, which suggests an important role of the holelike Fermi surface centered around the Γ point in the quasiparticle dynamics. We start with the two-dimensional single-band Hubbard model given by

$$H = \sum_{ij,\sigma} (t_{ij} c_{i\sigma}^{\dagger} c_{j\sigma} + \text{H.c.}) + U \sum_{i} n_{i\uparrow} n_{i\downarrow} - \mu \sum_{i\sigma} n_{i\sigma}, \qquad (1)$$

where t_{ij} denotes the hopping term (in the following, we will use t_1, t_2, t_3, and t_4 to denote the hoppings along the nearest to the fourth nearest neighbors), U the on-site Coulomb repulsion, and μ the chemical potential. To reproduce the large FS around the Γ point, we set the parameters (t_1, t_2, t_3, t_4) of the bare dispersion $\epsilon_{\mathbf{k}}$ to be $(-1, 0, 0, 0.2)$, where t_1 is set to be the unit hereafter. According to the numerical result for the bandwidth,[13,21] one can get $t_1 = 130$ meV. We note that the main feature of the bare dispersion is similar to that of the band with an a_{1g} character in the LDA calculation by Lee *et al.*[14]

The FLEX approximation is employed in our study, which has been applied to the two-dimensional Hubbard

model in the literatures.[22–25] As a self-consistent approximation, the FLEX approximation solves the Dyson's equation with a primarily random-phase approximation+ladder-type effective interaction self-consistently. Based on the scenario of the FLEX approximation, the self-energy is given by

$$\Sigma(k) = \frac{T}{N}\sum_{q} V_{eff}(k-q)G(q), \tag{2}$$

where

$$V_{eff}(q) = \frac{3}{2}U^2\chi_s(q) + \frac{1}{2}U^2\chi_c(q). \tag{3}$$

The spin susceptibility is

$$\chi_s(q) = \frac{\bar{\chi}(q)}{1 - U\bar{\chi}(q)}, \tag{4}$$

and the charge susceptibility is

$$\chi_c(q) = \frac{\bar{\chi}(q)}{1 + U\bar{\chi}(q)}, \tag{5}$$

with the irreducible susceptibility,

$$\bar{\chi}(q) = -\frac{T}{N}\sum_{k} G(k+q)G(k). \tag{6}$$

The electron Green's function is give by

$$G(k) = [i\omega_n - \epsilon_k - \Sigma(k)]^{-1}. \tag{7}$$

In the above equations, $k \equiv (\mathbf{k}, i\omega_n)$ and $q \equiv (\mathbf{q}, i\nu_n)$ are used, and T is the temperature. These equations are solved self-consistently, where $N=64\times 64$ $\mathbf{k}$-point meshes, and up to 2048 Matsubara frequencies $\omega_n=(2n+1)\pi T$ are taken. The electron density is determined by the chemical potential μ from the equation $\langle n\rangle = 1-\frac{2T}{N}\Sigma_k G(k)$.

As an important physical quantity related closely to the strength of the electronic correlations, the effective mass m^* is given by

$$\frac{m}{m^*} = Z\left(1 + \frac{m}{k_F}\frac{\partial}{\partial k}\,\mathrm{Re}\,\Sigma\,(k,0)|_{k=k_F}\right), \tag{8}$$

where

$$Z = \left(1 - \frac{\partial}{\partial \omega}\,\mathrm{Re}\,\Sigma\,(k_F,\omega)|_{\omega=0}\right)^{-1} \tag{9}$$

is the renormalization constant. The self-energy with real frequencies $\Sigma(\mathbf{k},\omega)$ is obtained with the Padé approximants,[26] which analytically continue $\Sigma(\mathbf{k},i\omega)$ from the Matsubara frequencies to the real-frequency axis. The ratio of the effective mass to the bare mass m^*/m with different on-site Coulomb repulsions U near the FS (point A in Fig. 1) is plotted in Fig. 2, where m^*/m increases monotonously with the increasing of U. It is noticeable that when U is less than 4, the enhancement of the effective mass is inapparent (<1.2). With a strong Coulomb repulsion ($U \geqslant 6 \approx 0.8$ eV), the effective mass is enhanced significantly. Comparing the calculated effective mass with the ARPES measurements (~ 2 for $x \sim 0.3$), we set $U\sim 6$ in the present simple model to reflect the strong correlation effect in $Na_{0.33}CoO_2$.[27] The strong electronic correlations are evident from Fig. 3(a), in which the spectral function of quasiparticles defined as $A(\mathbf{k},\omega) = -\frac{1}{\pi}\,\mathrm{Im}\,G(\mathbf{k},\omega)$ at the FS (point A in Fig. 1) is plotted. One can see that the sharp quasiparticle peak is suppressed with strong Coulomb repulsion. For $U=2$ and $T=0.1$, the spectral function shows a sharp peak near the Fermi energy. Increasing the Coulomb repulsion to $U=6$, the spectral function is broadened and the spectral weight at the Fermi level is reduced greatly.

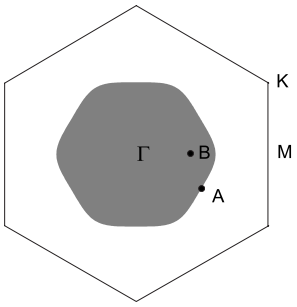

FIG. 1. The Fermi surface of $Na_{0.33}CoO_2$ for $(t_1,t_2,t_3,t_4) = (-1,0,0,0.2)$. The gray area denotes the unoccupied electron states. Point A near the Fermi surface indicates the $\mathbf{k}$ point where m^* is calculated.

For $U=6$, we now investigate the renormalization of the quasiparticle energy band. The renormalized band dispersion is determined by the position of the peak in $A(\mathbf{k},\omega)$. The calculated result at $T=0.1$ is shown in Fig. 3(b), where the solid and the dashed lines denote the renormalized and the bare energy bands, respectively. One can see that the bandwidth is compressed obviously due to the strong Coulomb interactions. From Fig. 3(b), one can determine that the bandwidth of the bare energy band is ~ 7.7 and the renormalized one is ~ 5.0, which give a band renormalization factor of 1.54. This is consistent with the ARPES measurements for $x=0.3$.[8] Moreover, we find that the band renormalization shows an anisotropy along the $\Gamma-K$ and $\Gamma-M$ directions, namely, the renormalization along the $\Gamma-K$ direction is

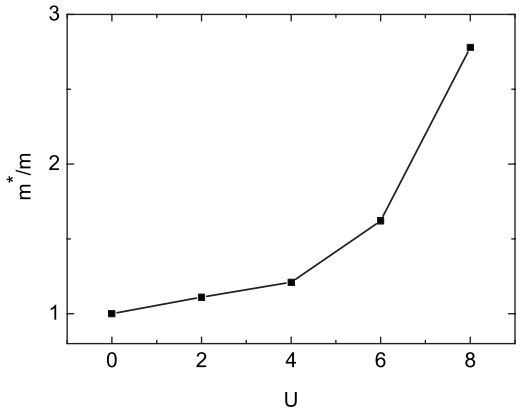

FIG. 2. The ratio of the effective mass to the bare mass m^*/m at point A as indicated in Fig. 1 versus the on-site Coulomb repulsion U at $T=0.1$.

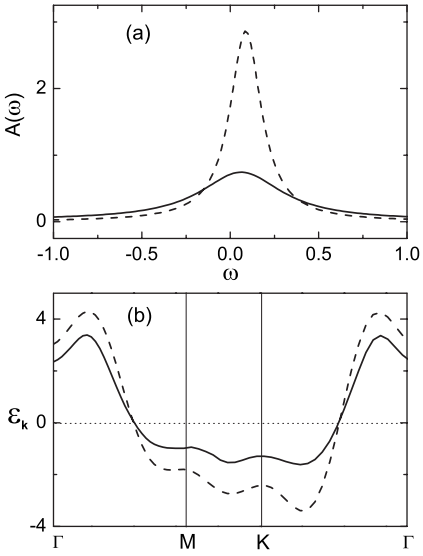

FIG. 3. (a) The effect of the on-site Coulomb repulsion on the spectral function at point A of Fig. 1. Solid line: $U=6$, $T=0.1$. Dashed line: $U=2$, $T=0.1$. (b) Solid line: the renormalized band dispersion for $U=6$ and $T=0.1$. Dashed line: the bare band dispersion. Dotted line: the Fermi energy.

stronger than that along the $\Gamma-M$ direction. A similar anisotropy has been found in the ARPES experiments for $x=0.6$,[7] though the experimental result seems stronger than what we get here. We note that the compound Na_xCoO_2 with $x=0.6$ is, in fact, in the range of the Curie-Weiss metal, in which the correlation is stronger than that in the paramagnetic metal with $x=0.3$. So a weaker anisotropy in the renormalization reported here is expected. This anisotropy originates from the nesting of the Fermi surface along the Γ-K direction, as shown in Fig. 1.

We now turn to address the weak pseudogap behavior. This is manifested in the suppression of DOS at the Fermi level. We present the ω dependence of DOS at different temperatures in Fig. 4. With the decrease of temperature from $T=0.7$ (dash-dotted) through $T=0.5$ (dotted) and $T=0.3$ (dashed) to $T=0.1$ (solid), a weak suppression of DOS near the Fermi energy is evident, suggesting the opening of a weak pseudogap. The weak pseudogap behavior is also manifested in the quasiparticle spectral function $A(\mathbf{k},\omega)$ which measures the probability to find quasiparticles at momentum $\mathbf{k}$ and frequency ω. As shown in Fig. 5(a), with the decrease of temperature (from the dashed line to the solid line), the spectral weight $A(\mathbf{k},\omega)$ at the $\mathbf{k}$-point B (shown in Fig. 1) is transferred away from the region around $\omega=0$, producing a weak secondary maximum at $\omega<E_F$. Thus, a weak pseudogap is formed.

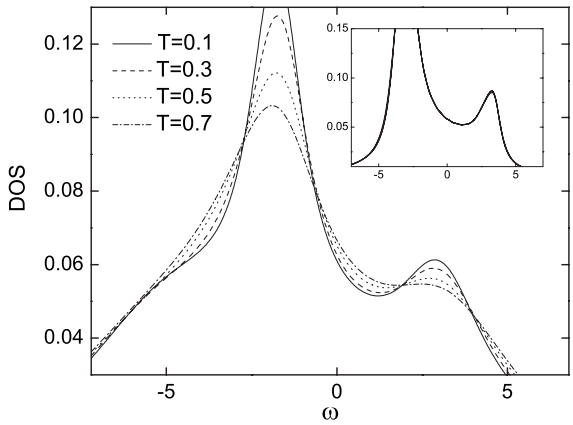

FIG. 4. The total density of states (DOS) versus energy for $U=6$. Solid line: $T=0.1$; dashed line: $T=0.3$; dotted line: $T=0.5$; and dash-dotted line: $T=0.7$. Inset: DOS plots for $U=2$ at $T=0.1,0.3,0.5,0.7$.

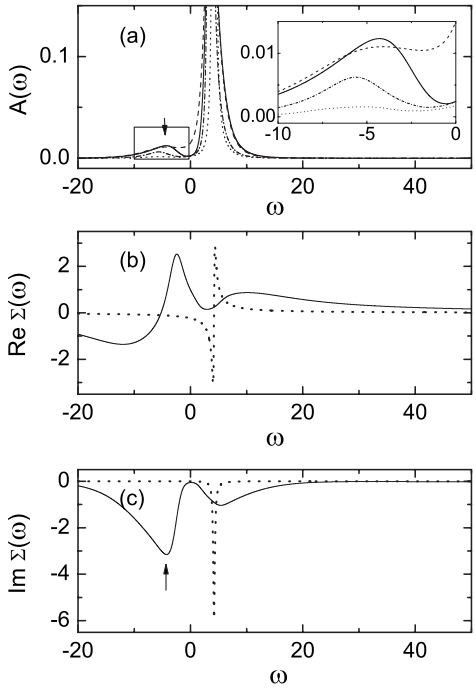

FIG. 5. (a) The energy dependence of the spectral function at the momentum indicated as point B in Fig. 1. Below the Fermi energy, there is a small peak in the spectral function for $U=6$ and $T=0.1$ (solid line). Dashed line: $U=6$ and $T=0.7$; dash-dotted line: $U=4$, $T=0.1$; and dotted line: $U=2$, $T=0.1$. The arrow points to the location of the secondary maximum. Inset: zoom-in view of the solid rectangle. [(b) and (c)] The real and the imaginary parts of the self-energy at $T=0.1$ for $U=6$ (solid) and $U=2$ (dotted). The arrow indicates the position of the extrema in $\mathrm{Im}\,\Sigma(\mathbf{k},\omega)$.

This weak pseudogap behavior is a consequence of strong Coulomb repulsion. To show this, we also present the results with a smaller $U=2$ at $T=0.1,0.3,0.5,0.7$ in the inset of Fig. 4. Different from the case of $U=6$, the density of states is not suppressed with the decreasing of temperature at all (in fact, there is no appreciable difference between them, so only one line can be seen from the figure). For a more detailed discussion, we also present the spectral function at the $\mathbf{k}$-point B (shown in Fig. 1) with a fixed temperature $T=0.1$ for $U=2$ (dotted), $U=4$ (dash-dotted), and $U=6$ (solid) in Fig. 5(a). It is seen that the spectral weight near the Fermi energy is suppressed, and consequently, a secondary maximum shows up gradually with the increase of Coulomb correlations. Note that since the depression and the secondary maximum disappears for $U=2$, no pseudogap is expected for this case and that for $U<2$. The *weak* pseudogap we refer here is based on

the observation that the spectral function consists of a peak and a weak secondary maximum (not a peak). In fact, the real part of the denominator of the Green's function has only one pole, which can be seen from the real part of the self-energy shown in Fig. 5(b). It is the extremum of the imaginary part of the self-energy around $\omega=-4$ that produces the weak maximum of the spectral function, as shown in Fig. 5(c). In the case of a smaller Coulomb repulsion U, such as $U=2$, a usual Fermi-liquid form of the self-energy is preserved [the dotted lines in Figs. 5(b) and 5(c)], so it gives a well-defined quasiparticle peak in the spectral function [the dotted line in Fig. 5(a)]. This secondary maximum might suggest a "shadow band",[28] which occurs when a short-range spin correlation is developed with the increase of Coulomb repulsion. Therefore, the weak pseudogap behavior reported here may be due to the spin fluctuation in the strong correlated regime.[29]

A similar weak pseudogap behavior was reported by Yada and Kontani[30] based on a multiorbital model with the absence of small hole pockets. Our results based on the single-band model provide further support for the sinking down of the small hole pockets. In our opinion, the agreement between the two models suggests that the multiorbital effect may play a minor role in the mechanism of the pseudogap formation.

In summary, we have studied the quasiparticle band renormalization and the pesudogap behavior in $Na_{0.33}CoO_2$ based on the single-band Hubbard model on a two-dimensional triangle lattice. The renormalization of the band structure and its anisotropy of the Γ-K and Γ-M directions have been elaborated. The estimated effective mass is consistent with the ARPES measurements. In the meantime, a weak pseudogap behavior is reproduced, which is explained as the result of the strong spin fluctuations. Our results are qualitatively consistent with experiments as well as the theoretical calculations based on a multiorbital model.

We thank Q.-H. Wang for helpful discussions. The work was supported by the NSFC (10525415, 10474032, and 10429401), the RGC grants of Hong Kong (HKU7045/04P and HKU-3/05C), the State Key Program for Basic Research of China (2006CB921800 and 2006CB601002), and MOE (NCET-04-0453).

[1] K. Takada, H. Sakurai, E. Takayama-Muromachi, F. Izumi, R. A. Dilanian, and T. Sasaki, Nature (London) **422**, 53 (2003).
[2] Y. Wang, N. S. Rogado, R. J. Cava, and N. P. Ong, Nature (London) **423**, 425 (2003).
[3] G. Baskaran, Phys. Rev. Lett. **91**, 097003 (2003).
[4] M. L. Foo, Y. Wang, S. Watauchi, H. W. Zandbergen, T. He, R. J. Cava, and N. P. Ong, Phys. Rev. Lett. **92**, 247001 (2004).
[5] R. Jin, B. C. Sales, P. Khalifah, and D. Mandrus, Phys. Rev. Lett. **91**, 217001 (2003).
[6] F. C. Chou, J. H. Cho, P. A. Lee, E. T. Abel, K. Matan, and Y. S. Lee, Phys. Rev. Lett. **92**, 157004 (2004).
[7] H.-B. Yang, S.-C. Wang, A. K. P. Sekharan, H. Matsui, S. Souma, T. Sato, T. Takahashi, T. Takeuchi, J. C. Campuzano, R. Jin *et al.*, Phys. Rev. Lett. **92**, 246403 (2004).
[8] H.-B. Yang, Z.-H. Pan, A. K. P. Sekharan, T. Sato, S. Souma, T. Takahashi, R. Jin, B. C. Sales, D. Mandrus, A. V. Fedorov *et al.*, Phys. Rev. Lett. **95**, 146401 (2005).
[9] T. Shimojima, K. Ishizaka, S. Tsuda, T. Kiss, T. Yokoya, A. Chainani, S. Shin, P. Badica, K. Yamada, and K. Togano, Phys. Rev. Lett. **97**, 267003 (2006).
[10] F. L. Ning, T. Imai, B. W. Statt, and F. C. Chou, Phys. Rev. Lett. **93**, 237201 (2004).
[11] T. Shimojima, T. Yokoya, T. Kiss, A. Chainani, S. Shin, T. Togashi, S. Watanabe, C. Zhang, C. T. Chen, K. Takada, T. Sasakir, H. Sakurai, and E. Takayama-Muromachi, Phys. Rev. B **71**, 020505(R) (2005).
[12] J. Hwang, J. Yang, T. Timusk, and F. C. Chou, Phys. Rev. B **72**, 024549 (2005).
[13] D. J. Singh, Phys. Rev. B **61**, 13397 (2000).
[14] K.-W. Lee, J. Kunes, and W. E. Pickett, Phys. Rev. B **70**, 045104 (2004).
[15] M. Z. Hasan, Y.-D. Chuang, D. Qian, Y. W. Li, Y. Kong, A. Kuprin, A. V. Fedorov, R. Kimmerling, E. Rotenberg, K. Rossnagel *et al.*, Phys. Rev. Lett. **92**, 246402 (2004).
[16] S. Zhou, M. Gao, H. Ding, P. A. Lee, and Z. Wang, Phys. Rev. Lett. **94**, 206401 (2005).
[17] K. Kuroki, Y. Tanaka, and R. Arita, Phys. Rev. Lett. **93**, 077001 (2004).
[18] K. Kuroki, Y. Tanaka, and R. Arita, Phys. Rev. B **71**, 024506 (2005).
[19] Y. Kobayashi, M. Yokoi, and M. Sato, J. Phys. Soc. Jpn. **72**, 2453 (2003).
[20] G.-Q. Zheng, K. Matano, D. P. Chen, and C. T. Lin, Phys. Rev. B **73**, 180503(R) (2006).
[21] J. Kunes, K.-W. Lee, and W. E. Pickett, in *Proceedings of the NATO Advanced Research Workshop on New Challenges in Superconductivity*, NATO Science Series II (Kluwer, Dordrecht, 2004).
[22] P. Monthoux and D. J. Scalapino, Phys. Rev. Lett. **72**, 1874 (1994).
[23] C.-H. Pao and N. E. Bickers, Phys. Rev. Lett. **72**, 1870 (1994).
[24] T. Dahm and L. Tewordt, Phys. Rev. Lett. **74**, 793 (1995).
[25] Z.-J. Yao, J.-X. Li, and Z. D. Wang, Phys. Rev. B **74**, 212507 (2006).
[26] H. J. Vidberg and J. W. Serene, J. Low Temp. Phys. **29**, 179 (1977).
[27] We note that similar Hubbard U value has been used in other theoretical studies, see, for example, K. Kuroki, S. Ohkubo, T. Nojima, R. Arita, S. Onari, and Y. Tanaka, Phys. Rev. Lett. **98**, 136401 (2007) and Ref. 14.
[28] J. J. Deisz, D. W. Hess, and J. W. Serene, Phys. Rev. Lett. **76**, 1312 (1996).
[29] We note that with stronger Coulomb repulsion, e.g., $U=10$, no qualitative difference is found. However, as expected, the secondary-maximum structure in $A(\mathbf{k},\omega)$ becomes more obvious as well as the pseudogap effect.
[30] K. Yada and H. Kontani, J. Phys. Soc. Jpn. **74**, 2161 (2005).